Double-exchange interaction in electron-doped $CaMnO_{3-\delta}$ perovskites

J. Briático, B. Alascio, R. Allub, A. Butera, A. Caneiro, M. T. Causa, and M. Tovar
Centro Atómico Bariloche and Instituto Balseiro, Comisión Nacional de Energía Atómica and Universidad Nacional de Cuyo, 8400 San Carlos de Bariloche, Río Negro, Argentina
(Received 4 December 1995; revised manuscript received 18 January 1996)

Removal of oxygen ions by thermogravimetric methods in $CaMnO_{3-\delta}$ ($0 \leqslant \delta \leqslant 0.34$) produces electron doping of the material and Mn^{4+} ions are reduced to a trivalent state. Electrical resistivity measurements in samples with controlled oxygen content show a strong increase of the conductivity for samples with $(3-\delta)=2.75$ and 2.84. The paramagnetic susceptibility at high temperatures can be described by a Curie-Weiss law with unusually large values for the Curie constant, which is also dependent on the oxygen stoichiometry. These results are interpreted in terms of ferromagnetic Mn^{3+}-Mn^{4+} spin clusters formed around the oxygen vacancies. An extension of the Anderson-Hasegawa Hamiltonian for the double-exchange interaction was made in order to understand the electric and magnetic behavior of these materials.
[S0163-1829(96)01221-0]

I. INTRODUCTION

Current interest in ABO_3 oxides with perovskite-type structure stems from the great variety of physical properties found in these substances. Recently, giant magnetoresistance has been observed in hole-doped $LaMnO_3$. The doping was performed through (i) the substitution of La^{3+} by divalent cations Ca, Sr, or Ba (Ref. 1) and (ii) internal doping with cation vacancies.[2] In both cases Mn ions are found in two valence states: Mn^{4+} ions are created from Mn^{3+} in $LaMnO_3$. A Zener double-exchange interaction has been proposed as the cause of the strong ferromagnetic interactions between Mn ions and of the metallic behavior found in these substances.[1,2]

In the case of the $CaMnO_3$ perovskite, where all the Mn ions are four valent and occupy sites with octahedral oxygen coordination, the introduction of oxygen vacancies also leads to a mixed valency family of compounds: $CaMnO_{3-\delta}$. The removal of an oxygen ion produces a reduction process where two neighboring Mn ions are converted to Mn^{3+}. When $\delta = 0.5$ all the Mn ions are trivalent and occupy sites with square pyramidal oxygen coordination.[3] $CaMnO_{3-\delta}$ belongs to the more general $ABO_{3-\delta}$ group, a particularly complex and phenomenologically rich group of nonstoichiometric compounds derived from the perovskite structure.[4] The physical properties of these compounds depend on the nature of the A and B cations and on the particular ordering of the oxygen vacancies that affects the oxygen coordination of the cations.[4] In the case of $CaMnO_{3-\delta}$, Reller *et al.*[5] have reported an electron-diffraction study of the perovskite superstructures and proposed the most likely vacancy structures compatible with the experimental data. Electrical resistivity measurements by Taguchi[6] for $\delta = 0$, 0.08, and 0.15 show an increase of the conductivity as δ increases. This observation may be associated with the mobility of the electrons left free in the reduction of the material. Early neutron-diffraction experiments[7] performed in $CaMnO_3$ show antiferromagnetic (AF) ordering at $T_N=110$–130 K. Magnetic susceptibilities were reported for the extreme compounds ($\delta = 0$ and 0.5) of the series. For $CaMnO_3$ a weak ferromagnetic component is present at $T \leqslant 130$ K,[8] while in $CaMnO_{2.5}$ the results were interpreted in terms of antiferromagnetic ordering at $T_N=350$ K.[3] It is interesting then to study simultaneously the magnetic and electric properties of this system in order to analyze to what extent the conductivity increase may be related to double-exchange interactions. With this purpose we have prepared samples of $CaMnO_{3-\delta}$, with carefully controlled oxygen content, for $0 \leqslant \delta \leqslant 0.34$. We present measurements of electrical resistivity extending the O-vacancy range studied in Ref. 6 to include samples richer in Mn^{3+}. We have also measured the magnetic susceptibility on the same samples covering a wide range of δ and temperatures not studied before.

II. EXPERIMENTAL PROCEDURES AND RESULTS

$CaMnO_3$ was prepared by the nitrate method. Metallic Mn and $CaCO_3$ were disolved in nitric acid and heated in air up to 800 °C. The synthetizing process was completed at 1400 °C for both powder and pressed pellets. The material obtained was slowly cooled to 600 °C and then quenched to room temperature. The reduction in H_2 at low temperatures ($\approx$ 300 °C) of sintered samples as indicated in Ref. 3 presented microcracks that made difficult the resistivity measurements. An alternative thermogravimetric method was then used. The samples were treated, in all the cases, at 1000 °C in a Cahn electrobalance with controlled Ar/O_2 atmospheres at different oxygen partial pressures P_{O_2}. Under these conditions, equilibrium was reached at compositions $CaMnO_{2.84}$ and $CaMnO_{2.66}$ for $P_{O_2}=10^{-2}$ atm and 10^{-4} atm, respectively. $CaMnO_{2.75}$ was obtained with $P_{O_2}=10^{-3}$ atm by quenching the sample when the desired composition was reached. It should be noted that full equilibrium was not achieved in this case. The oxygen content of the oxidized compound was established by hydrogen reduction as explained in Ref. 3 estimating in 0.5% the composition error in the whole series.

The samples were characterized by x-ray powder diffraction. The spectrum for $CaMnO_3$ was virtually free from im-

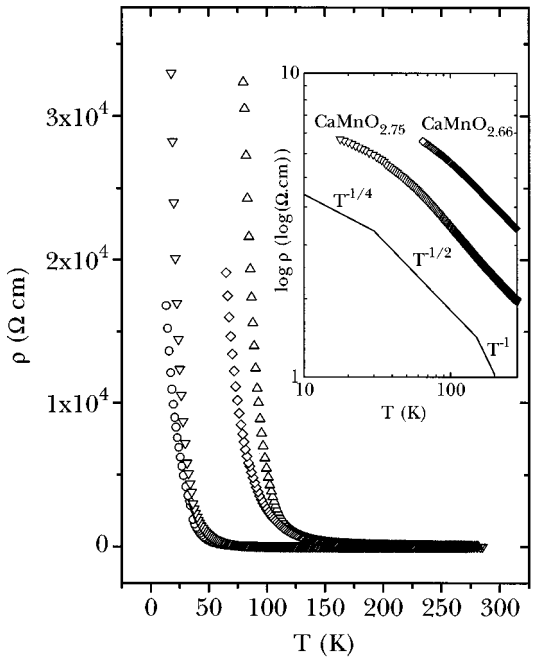

FIG. 1. Electrical resistivity vs T for (△) $CaMnO_3$, (○) $CaMnO_{2.84}$, (▽) $CaMnO_{2.75}$, and (◇) $CaMnO_{2.66}$. Inset: log(ρ) vs T for $CaMnO_{2.66}$ (◇) and $CaMnO_{2.75}$ (▽). Solid lines represent T^{-1}, $T^{-1/2}$, and $T^{-1/4}$ dependence for log(ρ).

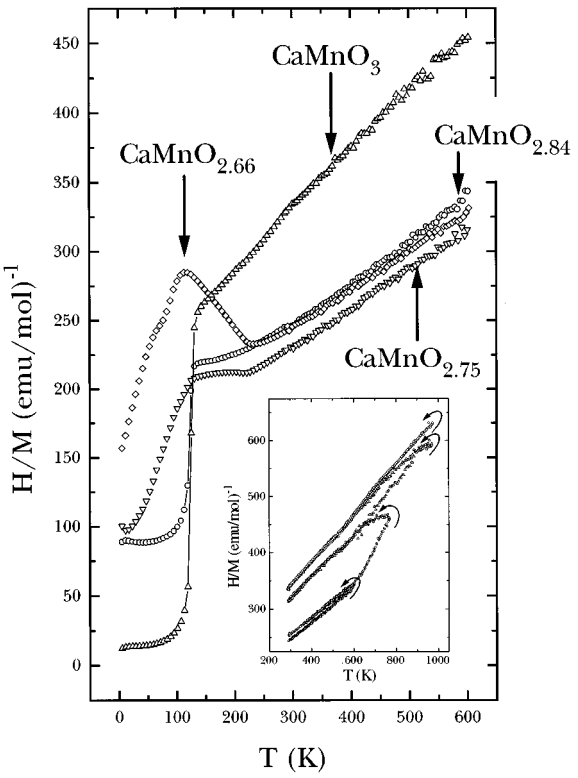

FIG. 2. χ^{-1} vs T for $CaMnO_{3-\delta}$ series. In the inset, the irreversible behavior reflects the *in situ* reoxidation of $CaMnO_{2.84}$ above $T \approx 600$ K.

purities phases and is coincident with that reported for single crystals in Ref. 3. It corresponds to a pseudotetragonal structure with lattice parameters $a \approx b \approx \sqrt{2}a_c$, $c \approx 2a_c$, where $a_c \approx 3.724$ Å is the ideal size of the undistorted perovskite cell. The spectra for the reduced samples with $(3-\delta)=2.84$ and 2.75 indicate the presence of crystallographic phases with larger distortions of the original perovskite structure, as found in previous work (Refs. 5,9). For $(3-\delta)=2.66$, a new phase was observed whose x-ray pattern shows major differences with those of the less reduced samples.

The electrical resistivity was measured by a standard four probe method in the temperature range 20–300 K. Magnetization was measured with a Faraday balance magnetometer in the range 300–1000 K and with a superconducting quantum interference device (SQUID) magnetometer between 5 K and 300 K.

In Fig. 1 we show the temperature dependence of the electric resisitivity, ρ vs T, for the $CaMnO_{3-\delta}$ series. In all cases $\rho(T)$ increases as the temperature diminishes, while at any fixed temperature we have found an important increase of the conductivity with the O-vacancy doping. A minimum of $\rho(T)$ was reached for an oxygen content between 2.75 and 2.84. The temperature dependence of log$\rho(T)$ is not well represented by a T^{-1} law even at high temperatures. At low temperatures ($T<30$ K) a $T^{-1/4}$ law seems to describe better the experimental results, as shown in Fig. 1, in agreement with the behavior found in Ref. 6.

Around and above room temperature ($300\ \text{K} \leqslant T \leqslant 600$ K) the magnetic susceptibility for all samples measured follows a Curie-Weiss law, $\chi = C/(T+\Theta)$ (see Fig. 2). The Curie constant $C(\delta)$, obtained in the 300–600 K range, depends on the oxygen content and increases with δ as shown in Fig. 3. We have determined a large antiferromagnetic value for the Curie-Weiss temperature ($\Theta \approx 500$ K) for all samples. Above $T \approx 600$ K the magnetic susceptibility deviates from a Curie Weiss law and hysteretic behavior is observed in the $\chi(T)$ vs T curves. Simultaneous measurements (in the Faraday

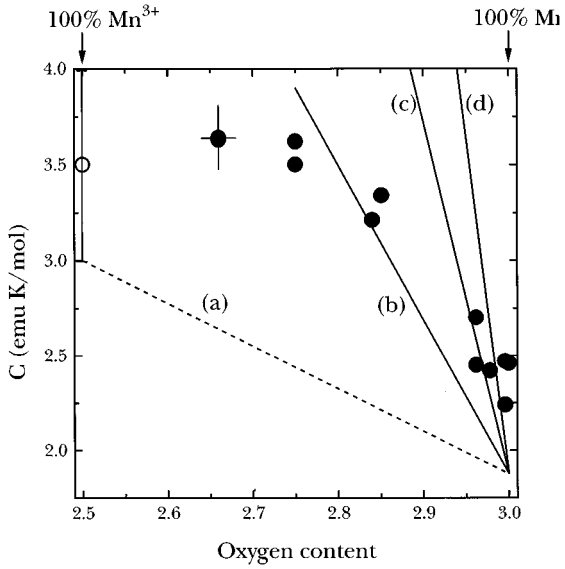

FIG. 3. Curie constant vs oxygen content $(3-\delta)$. The open circle is an estimation from Ref. [3]. The dashed line (a) shows calculated Curie constant for mixtures of weakly interacting Mn^{3+} and Mn^{4+} ions. The solid lines correspond to ferromagnetic clusters where one Mn^{3+} is strongly coupled to one (b), two (c), and threee (d) Mn^{4+} ions.

balance) of the changes in the sample mass indicate that a reoxidation process takes place at these temperatures even for very low values of P_{O_2} (see Fig. 2). A sample of $CaMnO_{2.84}$ reached a final composition $CaMnO_{3.00}$, after warming up to 1000 K. Oxidized samples retained their oxygen content when cooled to room temperatures. This *in situ* heat treatment of the $CaMnO_{2.84}$ sample allowed the determination of $C(\delta)$ for $2.84 \leqslant (3-\delta) \leqslant 3.00$.

At low temperatures a weak ferromagnetic component m_{WF} in the magnetization was detected in all the studied samples for $T \leqslant 125$ K. The high-field susceptibility presents a rounded maximum, which would indicate AF ordering, at temperatures ranging from 110 K for $CaMnO_3$ to 240 K for $CaMnO_{2.66}$. The saturation value of $m_{WF} \approx 0.04\mu_\beta$ for $\delta = 0$ agrees with Ref. 8. For $\delta > 0$ we obtained decreasing values of m_{WF}, being $m_{WF} \approx 0.01\mu_B$ for $3-\delta = 2.84$. For $3-\delta = 2.75$ and 2.66 a saturation value is not reached at $T > 5$ K as is shown in Fig. 2. In summary we have not found any relation between this low temperature weak ferromagnetic behavior and the electrical conductivity on the same samples. Therefore the observed weak ferromagnetic behavior does not seem to be connected to the double-exchange mechanism in any way.

III. DISCUSSION

To understand the effect of oxygen vacancies in these materials we study first a simple extension of the model for double exchange proposed by Anderson and Hasegawa,[10] where the diagonal energies (ϵ_i) at the two Mn sites are different according to the oxygen environment. We assume that the energy ϵ_2 for the regular octahedral coordination is larger than ϵ_1, which corresponds to the square pyramidal coordination (one oxygen vacancy in the octahedron).

The corresponding Hamiltonian is

$$H = \sum_{i,\sigma} \epsilon_i n_{i\sigma} - t \sum_{\sigma} (c^{\dagger}_{1\sigma} c_{2\sigma} + \text{H.c.}) - J \sum_i \vec{S}_i \vec{\sigma}_i + U \sum_i n_{i\uparrow} n_{i\downarrow} ,$$

where t is the hopping energy, J is the intraatomic exchange energy (we take $J > 0$ and $J \gg t$) , and U is the Coulomb repulsion. $c_{i\sigma}$ annihilates an electron of spin σ at site i and $n_{i\sigma} = c^{\dagger}_{i\sigma} c_{i\sigma}$. $\vec{S}_i$ and $\vec{\sigma}_i$ are the ionic and itinerant spin operators, respectively. $S = 3/2$ corresponds to Mn^{4+} ions in high-spin configuration.

We further assume $U \to \infty$ to inhibit the possibility of forming Mn^{2+} ions when electrons are added to the system. For a pair of Mn ions the zero-particle states correspond to noninteracting Mn^{4+} ions and the two-particle states correspond to noninteracting Mn^{3+} ions. The one-particle states correspond to mixed valency states where the double-exchange mechanism operates. As a consequence, the ground state depends on the local spin configuration. If the local spins are parallel to each other, the added electron spin is also parallel to them (total spin $2S + 1/2$) and the probability to find it in any of the sites is finite. If the local spins are antiparallel, the added electron remains more localized in the lower-energy site with its spin parallel to the local spin (total spin 1/2). The energy difference between the antiparallel and parallel configurations, neglecting terms in $(t/J)^2$, is given by $\Delta = \sqrt{(\epsilon_1 - \epsilon_2)^2/4 + t^2} - \sqrt{(\epsilon_1 - \epsilon_2)^2/4 + (t/4)^2}$. This energy difference, as in the case of the Anderson-Hasegawa Hamiltonian, favors the alignment of the spins of neghboring atoms and at the same time favors hopping of the added electron between them. One should notice, however, that $\Delta \to 0$ when $(\epsilon_1 - \epsilon_2)/t \to \infty$ making the double-exchange mechanism ineffective when the energy difference between sites is large.

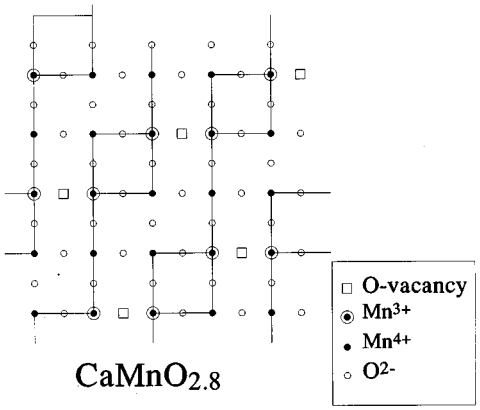

FIG. 4. Oxygen vacancies ordering in the ab plane for $CaMnO_{2.84}$ as proposed in Ref. 5. The lines indicate possible paths for electron propagation.

Having this picture in mind, we can imagine first, ignoring t, that the two nearest-neighbor Mn sites to an oxygen vacancy will be occupied by the two electrons that the removed oxygen ion leaves behind. In the absence of hopping, this configuration is expected to be stable since the pyramidal oxygen coordination presents lower diagonal energy. Turning on the hopping term, the double-exchange mechanism will act to connect them with their nearest-neighbor Mn^{4+} ions through oxygen bridges. Due to the ferromagnetic effective interaction, two high-spin clusters will be formed, where the extra electrons move relatively free.

We propose that these spin clusters are the origin of the high values of the Curie constants found in the oxygen defective samples. For isolated clusters the maximum effective spin value is $6S + 1/2$. We compare in Fig. 3 the expected Curie constant for $CaMnO_{3-\delta}$ samples, assuming (a) paramagnetic and weakly interacting Mn^{3+} and Mn^{4+} ions and (b) Mn^{3+}-Mn^{4+} ions coupled in clusters of two, three, and four sites, with total spin of 7/2, 5, and 13/2, respectively. Notice that the experimental data are better described in terms of clusters than as a weakly interacting mixtures of Mn^{3+} and Mn^{4+} ions. When the vacancy concentration increases, and consequently the density of clusters, the electrical resistance of the whole samples is expected to be lowered due to hopping of the electrons between clusters. The temperature dependence of the resistance of the $\delta = 1/6$ and 1/4 suggests that this hopping is thermally activated.

We can go further in this direction: According to Reller *et. al.*,[5] the oxygen vacancies in $CaMnO_{3-\delta}$ form well-ordered structures for $\delta \simeq 1/6, 1/4, 1/3$ with rows of vacancies along the c axis, as shown in Fig. 4 for the compound $CaMnO_{2.84}$. The ordering of vacancies leads in a natural

way to the crystallographic ordering of Mn^{3+} and Mn^{4+} ions. Inspection of Fig. 4 shows that the Mn^{3+} and Mn^{4+} ions form one-dimensional paths for electron propagation in the ab plane. Similar chains of alternating Mn^{3+} and Mn^{4+} ions can also be identified for $(3-\delta)=2.75$ and 2.66. However, the density of Mn^{3+}-Mn^{4+} chains, and thus the expected conductivity, is maximum for the $CaMnO_{2.84}$ structure. The conductivity goes to zero for $\delta = 0$ and 0.50. In order to explore the validity and consequences of these ideas it is necessary to grow single crystals with precise content of vacancies.

The effect of substitution of Ca ions by La, forming $La_{1-x}Ca_xMnO_3$, can also be understood on the basis of this picture.[11] One can expect that the Mn ion nearest neighbors of La ions will have different diagonal energies than the rest. However, each La ion will have eight Mn nearest neighbors instead of two as is the case of oxygen vacancies, and then the energies differences will be smaller. These two factors favor the propagation of the added electrons and can lead to the metallization of the disordered alloys.

ACKNOWLEDGMENTS

We acknowledge partial support from the Commission of the European Communities DG-XII-G (Contract No. CI1*CT92-0087) and the Consejo Nacional de Investigaciones Científicas y Técnicas (CONICET) of Argentina.

[1] See, for example, Y. Tokura, A. Asamitsu, G. Kido, and N. Furukawa, J. Phys. Soc. Jpn. **63**, 3931 (1994).
[2] S. Sundar Manoharan, Dhananjay Kumar, M. S. Hegde, K. M. Satyalakshmi, V. Prasad, and S. V. Subramanyam, J. Solid State Chem. **117**, 420 (1995).
[3] K. R. Poeppelmeier, M. E. Leonowicz, and J. M. Longo, J. Solid State Chem. **44**, 89 (1982).
[4] M. T. Anderson, J. T. Vaughey, and K. R. Poeppelmeier, Chem. Mater. **5**, 151 (1993).
[5] A. Reller, J. M. Thomas, and D. A. Jefferson, Proc. R. Soc. London A **394**, 223 (1984).
[6] H. Taguchi, Phys. Status Solidi A **88**, K79 (1985).
[7] E. O. Wollan and W. C. Koehler, Phys. Rev. **100**, 545 (1955).
[8] G. H. Jonker, Physica **22**, 707 (1956).
[9] C. C. K. Chiang and K. R. Poeppelmeier, Mater. Lett. **12**, 102 (1991).
[10] P. W. Anderson and H. Hasegawa, Phys. Rev. **100**, 675 (1955).
[11] J. Mazzaferro, C. A. Balseiro, and B. Alascio, J. Phys. Chem. Solids **46**, 1339 (1985); R. Allub and B. Alascio (unpublished).